Phase Velocities of Long-Period Surface Waves and Structure of the Upper Mantle

1. Great-Circle Love and Rayleigh Wave Data[1]

M. NAFI TOKSÖZ[2] AND DON L. ANDERSON

Seismological Laboratory, Division of Geological Sciences
California Institute of Technology, Pasadena

Abstract. New long-period dispersion data are obtained from the surface waves generated by the Alaska earthquake of March 28, 1964, and recorded at Isabella, Kipapa, and Stuttgart. Digital techniques were used to isolate phases and determine spectrums over the period band 80 to 670 seconds. Available phase velocity data are now accurate enough to permit us to discuss regional variations which can be attributed to heterogeneity of the upper 400 km of the mantle. Average phase velocities are markedly affected by the character of the continental fraction of the path. Shield areas raise the average phase velocity; tectonic and mountainous areas have the opposite effect. The tectonic-shield distinction is as important as the more obvious continental-oceanic distinction. An average mantle structure, designated CIT 12, is determined for the Mongolia-Pasadena composite great-circle path. The major features of this new mantle model are similar to those determined for the New Guinea–Pasadena great-circle path (model CIT 11), namely, a pronounced and deep low-velocity zone and two discontinuities in the upper mantle at depths near 350 km and 700 km. The two models differ in a way that suggests lower average shear velocities under tectonic regions than under shield areas to depths of the order of 400 km.

Introduction. Seismic surface waves have proved to be a powerful tool in the study of the crust and upper mantle. The dispersion of short-period surface waves—the so-called crustal waves—is being used for studying average crustal structure in various regions of the world. Regional variations in crustal structures are quite pronounced. Observations of longer-period (or mantle) waves are more limited because of the requirements of instrumentation and source size, but they have been sufficient to permit us to discuss average properties of the mantle and to suggest the possibility of mantle differences to depths of the order of hundreds of kilometers. Great improvements have been made in both the quality and the quantity of phase velocity data and in the means of interpretation in terms of mantle velocity structures. The accuracy of the measured phase velocities is now such that we can detect small variations between different paths.

In this study we measured phase velocities of mantle Love and Rayleigh waves from the Alaska (Prince William Sound) earthquake of March 28, 1964, over several great-circle paths. These velocities are compared with previous measurements from a number of other large earthquakes. A structure for the upper mantle is determined which satisfies the composite path data. This can be considered a mean earth structure, since the raw data include oceanic and continental segments.

By combining data from different composite great-circle paths it is possible to estimate dispersion curves appropriate to a 'pure path.' We interpreted the composite-path data in terms of segments which we designate *oceanic, shield,* and *mountain-tectonic.* The structural models associated with these pure paths and the implications of the regional variations will be discussed in a later paper.

Phase velocity measurements. Determination of mantle velocity structures depends on accurate phase and group velocity data over a relatively broad frequency band. The phase velocities are computed by measuring the phase

[1] Contribution 1359, Division of Geological Sciences, California Institute of Technology, Pasadena.

[2] Now at the Department of Geology and Geophysics, Massachusetts Institute of Technology, Cambridge.

TABLE 1. List of Stations and the Usable Phases from the Prince William Sound Earthquake

Station	Coordinates		Epicentral Distance, km	Great-Circle Path, km	Available Phases
	Latitude	Longitude			
Isabella	35.66°N	118.47°W	3489	40018	G_2, G_4, R_2, R_4, R_3, R_5
Kipapa	21.42°N	158.05°W	4477	40010	G_1, G_3, G_5
Stuttgart	48.77°N	9.19°E	7651	40010	G_4, G_6

delay of each Fourier component of the wave over a known distance. This can be done exactly by using the Fourier phase spectrums [*Satô*, 1958; *Toksöz and Ben-Menahem*, 1963] or approximately by measuring the time delay directly from the seismogram [*Brune et al.*, 1961].

The phase velocities can be determined from a single station by using two successive passages of the same wave train, such as $G_1 - G_3$ or $R_2 - R_4$ [*Satô*, 1958; *Toksöz and Ben-Menahem*, 1963]. This technique has a distinct advantage over a multiple-station method because the errors due to variations of instrument responses and nonuniformity of initial phases of the source function along different azimuths are avoided. Furthermore, the great distances involved in this type of study lead to an improvement in accuracy over what can be obtained for shorter distances. The phase velocity c at period T is given by

$$c(T) = \frac{\Delta}{\delta t + T[\delta\phi(T) + N - \frac{1}{2}]} \qquad (1)$$

where Δ = length of great circle, $\delta t = t_{n+2} - t_n$, and $\delta\phi(T) = \phi_{n+2}(T) - \phi_n(T)$. t_{n+2} and t_n are the initial times of the Fourier windows; ϕ_{n+2} and ϕ_n are the phase delays relative to the beginnings of the windows, N is an integer, and $-\frac{1}{2}$-circle phase shift is due to the two extra polar passages with a $\pi/2$ phase shift per polar passage.

The Alaska earthquake of March 28, 1964, generated Love and Rayleigh waves of very long period. Unfortunately, at most stations the recordings were off scale and seismogram traces could not be recovered. We were able, however, to find three stations with usable records. The pertinent station information is listed in Table 1. California Institute of Technology's Isabella and Kipapa stations are equipped with strain seismographs. The station at Stuttgart is a USCGS worldwide standard station. At Kipapa there was only one component of the strain instrument, and only Love waves were recorded. The lack of Rayleigh waves is attributed to the source-space function of the earthquake. At Stuttgart the only waves we could separate were from a horizontal-component record which is nearly transverse to the great-circle direction. The separated wave trains from these two stations are shown in Figures 1 and 2.

At Isabella there were usable strain recordings of both Love and Rayleigh waves. However, the successive odd- and even-order passages (i.e., G_2 and G_3) interfered, and the utilization of these waves required separation of the interfering wave trains. A time-varying filtering technique developed by W. Pilant (private communication, 1963) was used in this separation. The upper and lower cutoff frequencies are of a digital bandpass filter changed at specified points along the time series. The varying passband is adjusted so that at a given time it covers only the segment of the desired wave train.

The application of this filter is illustrated in Figures 3 and 4. The smooth curves represent estimates of frequency versus travel time for Love waves from Alaska to Isabella. These curves are computed using average values of theoretical and experimental group velocity curves. The passbands of the filters, shown as solid and dashed lines bordering the smooth travel-time curves, are adjusted to eliminate the interference. The need for this procedure is especially apparent in the case of $G_4 - G_5$ (Figure 4) if velocities are to be measured for periods longer than 300 sec.

The success of such time-dependent filtering is demonstrated in Figures 5 (original seismogram) and 6 (filtered traces), where G_2 and G_4 phases recorded at Isabella are cleared of

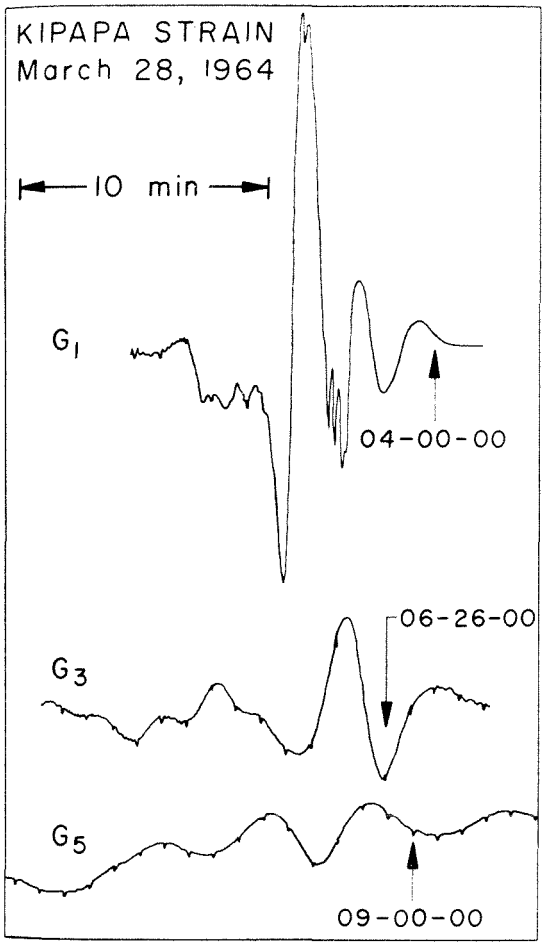

Fig. 1. Love waves from the Alaska earthquake recorded at Kipapa.

the G_3 and G_5 interferences. The same technique was applied to separate the Rayleigh wave trains before Fourier analysis. At Kipapa the amplitudes of even-order waves (G_2, G_4) were very small because of source directivity [*Toksöz et al.*, 1965], and the interference did not constitute a problem. The same was true for Stuttgart because of the favorable epicentral distance. Only bandpass filtering was used in analyzing the records of these stations.

The phase velocities were determined from the Fourier phase spectrums of filtered traces using equation 1. An example of the spectrums is shown in Figure 7. The computed phase velocities are tabulated in Table 2. Velocities from our previous measurements [*Toksöz and Ben-Menahem*, 1963] are also listed in the same table for easy reference and comparison. The period range of the data is between 666 and 80 sec, although no single determination covers the whole range. The distribution of great-circle paths (Figure 8) shows that most regions of the world are traversed. The Love wave data are more abundant, and the coverage is much better than for Rayleigh waves.

Regional variations. Comparing these velocities for different great-circle paths, we see that the agreement between velocities is very good (better than 0.5%) where the paths are close. Where the paths are quite different, there are considerable differences in the values of phase velocities, and these are more pronounced

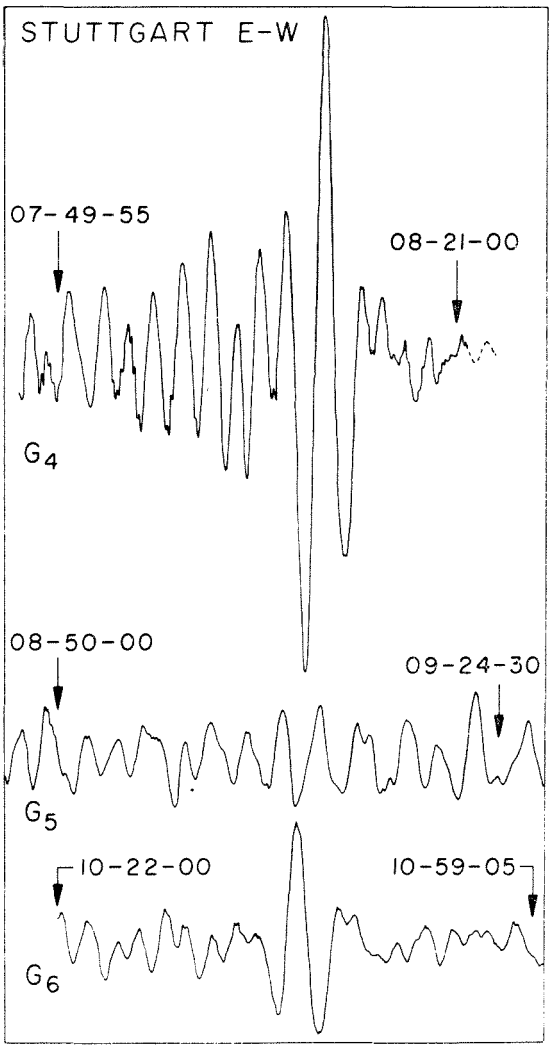

Fig. 2. Love waves recorded at Stuttgart. Note the relatively small amplitude of G_5 due to source directivity.

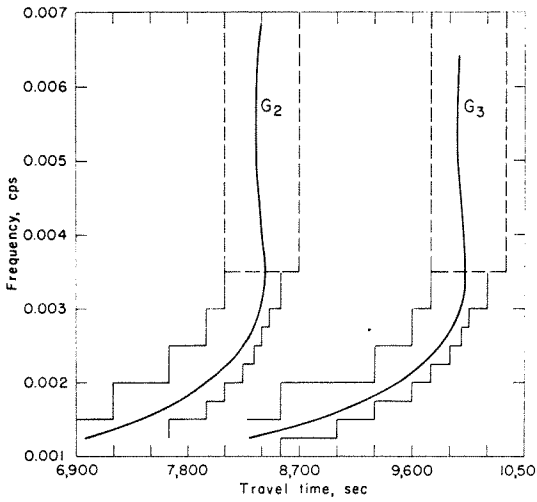

Fig. 3. Frequency–travel-time plot for G_2 and G_3 at Isabella.

at the shorter periods. The very obvious conclusion regarding the upper mantle is that the structure and the velocities vary laterally.

Interpretation of the phase velocity data given in Table 2 in terms of upper mantle structures is a complex problem. Each path is heterogeneous, involving different geological and physiological provinces such as oceanic and continental areas. For example, the New Guinea–Pasadena great-circle path is predominantly oceanic. The Alaska (1964) to Stuttgart (note that Kipapa lies on the same path) and the Alaska (1958) to Wilkes paths are quite different from the remaining six paths.

In part 2 [*Anderson and Toksöz*, 1966] we will discuss the implications of this composite

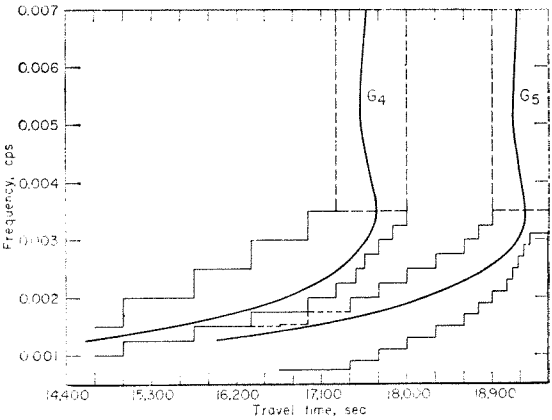

Fig. 4. Frequency–travel-time plot for G_4 and G_5 at Isabella.

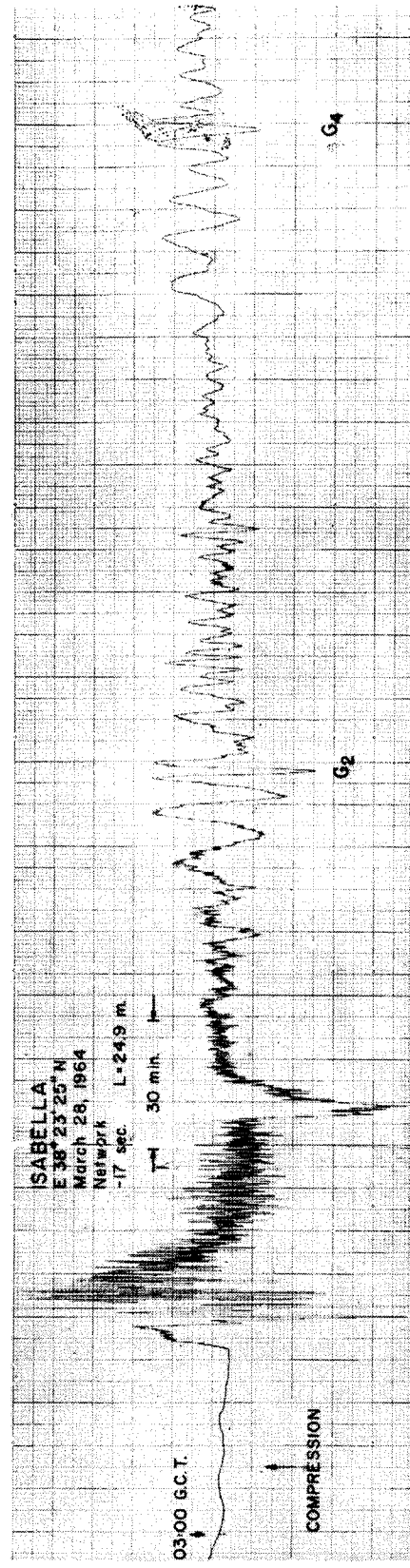

Fig. 5. Isabella strain seismogram of Alaska earthquake.

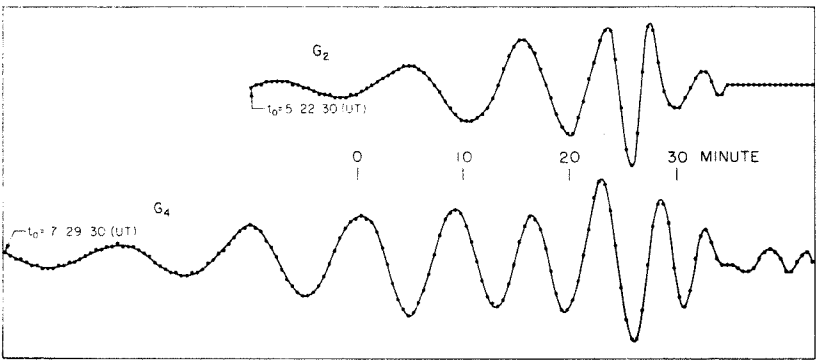

Fig. 6. G_2 and G_4 traces from Figure 5 filtered with the time-varying filter to remove interference of odd-order passages.

path data in terms of regional variations in the upper mantle. For the present we will be content with a qualitative discussion of gross regional trends.

The distribution of the paths over the earth is not dense enough, nor uniform enough, to warrant an interpretation along the lines suggested by *Backus* [1964] for determining regional phase velocities. However, it is possible to extract some information about regional differences in phase velocity from these data. The most obvious parameter that can be assigned to the various great-circle paths is the amount of ocean traversed. The following oceanic percentages, excluding continental shelves, have been determined: Alaska–Wilkes, 75%; New Guinea–Pasadena, 71%; Alaska–Isabella, 61%; Mongolia–Pasadena, 59%; and Alaska–Kipapa–Stuttgart, 52%. Any great-circle path is, of course, primarily oceanic. Note, however, that the phase velocity data in Table 2 are not ordered, as we might expect, with phase velocity increasing as the fraction of ocean along the path increases. The Alaska–Kipapa–Stuttgart path, for instance, has the largest phase velocities and the smallest fraction of ocean of any path considered. The Alaska–Wilkes and New Guinea–Pasadena paths have the largest oceanic portions, but their phase velocities are intermediate. Clearly, the percentage of ocean, although it is the major part of each path, does not, by itself, control the ordering of the phase velocity curves. We are therefore forced to consider other differences among the paths. There are several possibilities. The oceanic mantle itself may not be uniform. We would not expect ocean basins, deep trenches, rises, and mid-ocean ridges to be underlain by identical mantle. However, the oceanic parts of the paths considered here do not differ appreciably in their content of the various oceanic structures. We do not therefore feel justified, at present, in subdividing the oceanic paths. The continents, also, are not uniform. The simplest subdivision is into stable shield areas and tectonic areas—in the latter we will include mountainous regions as well as earthquake and volcanic belts. These percentages are listed in Table 3. The percentages for shield and tectonic paths differ significantly from path to path. The highest velocity path, Alaska–Kipapa–Stuttgart, has a remarkable

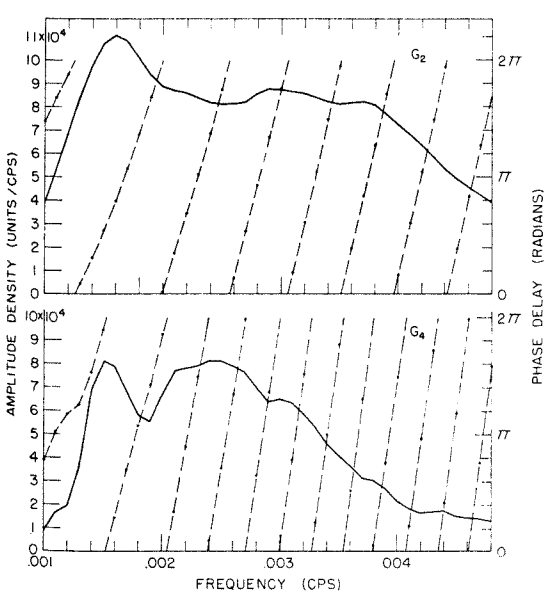

Fig. 7. Amplitude and phase spectrums of filtered waves shown in Figure 6.

TABLE 2. Phase Velocities for Various Periods and Great-Circle Paths

Frequency, cps	Period, sec	Phase Velocity, km/sec							
		Alaska–Isabella *G*	Mongolia–Pasadena *G*	Alaska*–Wilkes *G*	New Guinea–Pasadena *G*	Alaska–Kipapa *G*	Alaska–Stuttgart *G*	Alaska–Isabella *R*	Mongolia–Pasadena *R*
0.0015	666.67	6.250				6.230		7.331	
0.0016	625.00	6.133				6.140		7.029	
0.0017	588.24	6.038				6.047		6.797	
0.0018	555.56	5.970				5.947		6.643	
0.0019	526.32	5.919						6.501	
0.0020	500.00	5.861						6.402	
0.0021	476.19	5.797						6.311	
0.0022	454.55	5.728						6.211	
0.0023	434.78	5.660						6.115	
0.0024	416.67	5.599						5.999	
0.0025	400.00	5.548						5.892	
0.0026	384.62	5.501	5.506					5.836	
0.0028	357.14	5.415	5.403				5.447	5.685	5.627
0.0030	333.33	5.330	5.317	5.324				5.500	5.485
0.0032	312.50	5.262	5.244	5.274		5.284	5.285	5.380	5.358
0.0034	294.12	5.201	5.181	5.221				5.245	5.229
0.0036	277.78	5.146	5.126	5.171		5.175	5.174	5.096	5.118
0.0038	263.16	5.095	5.078	5.123	5.113			5.005	5.003
0.0040	250.00	5.059	5.036	5.078	5.074	5.086	5.088	4.912	4.913
0.0042	238.10	5.023	4.998	5.037	5.038			4.822	4.817
0.0044	227.27	4.992	4.965	5.001	5.007	5.016	5.015	4.744	4.744
0.0046	217.39	4.958	4.934	4.968	4.973			4.671	4.682
0.0048	208.33	4.924	4.907	4.940	4.953	4.960	4.960	4.598	4.612
0.0050	200.00	4.890	4.882	4.914	4.930			4.531	4.568
0.0052	192.31	4.864	4.860	4.891	4.909	4.914	4.920		4.523
0.0056	178.57	4.820	4.821	4.851	4.874	4.878	4.884		4.434
0.0060	166.67	4.788	4.789	4.818	4.840	4.831	4.847		4.370
0.0064	156.25	4.767	4.760	4.792	4.812	4.806	4.815		4.316
0.0068	147.06	4.714	4.736	4.770	4.786	4.793	4.793		4.279
0.0072	138.89		4.713	4.752	4.765	4.769	4.776		4.255
0.0076	131.58		4.693	4.736	4.745	4.742	4.751		4.234
0.0080	125.00		4.674	4.722	4.728		4.710		4.203
0.0084	119.05		4.657	4.713	4.714				
0.0088	113.64		4.642	4.699	4.700				
0.0092	108.70		4.628	4.687	4.688				
0.0096	104.17		4.615	4.677	4.677				
0.0100	100.00		4.603		4.668				
0.0104	96.15		4.592		4.659				
0.0108	92.59		4.582		4.651				
0.0112	89.29		4.572		4.643				
0.0116	86.21		4.564		4.636				
0.0120	83.33		4.555		4.622				
0.0124	80.64				4.609				

* Alaska earthquake of July 10, 1958.

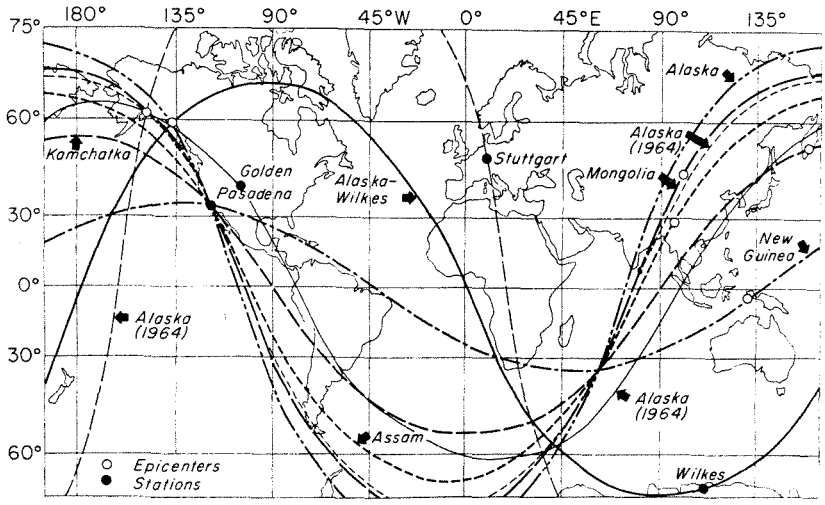

Fig. 8. Great-cycle paths over which mantle Love and/or mantle Rayleigh wave dispersion data are available.

42% stable shield fraction along the entire great circle. The lowest velocity paths, Alaska–Isabella and Mongolia–Pasadena, both have less than 6% shield and more than 35% tectonic paths. The intermediate phase velocity data involve paths with intermediate fractions of both shield and tectonic components. Differences are significant to periods as long as at least 350 sec, and probably much longer. The implication is clear—the distinction between stable shield areas and mountainous-tectonic areas is as important and fundamental as the more obvious distinction between oceans and continents, and this distinction must extend to great depths in the mantle.

If we assume that the over-all phase delay of a surface wave is a linear function of the individual phase delays over the various segments of the paths, we can determine the phase velocity appropriate for each region. By using this procedure we ignore the possibility of a phase shift at the boundaries of the regions.

This procedure yielded the three pure-path Love wave dispersion curves labeled shield, ocean, and mountain-tectonic in Figure 9. The pure-ocean curve is roughly midway between the two continental curves. The difference between a shield area and a tectonic area is now strikingly demonstrated, and implies significant velocity differences to depths of the order of at least 400 km. In part 2 we will describe, in detail, structures which were designed to satisfy the pure-path data, thereby quantifying the above discussion. In the next section we determine an average structure which satisfies the Love and Rayleigh wave composite dispersion data over the six paths clustered around the Mongolia–Pasadena great circle.

Composite mantle model. A mantle model was determined by use of the *earth-stretching approximation* [*Anderson and Toksöz,* 1963] and the universal dispersion tables [*Anderson,*

TABLE 3. Path Parameters

	New Guinea–Pasadena, %	Alaska–Isabella, %	Mongolia–Pasadena, %	Alaska–Wilkes, %	Alaska–Kipapa-Stuttgart, %
Oceanic	71	61	59	75	52
Tectonic	11	39	35	1	5
Shield	18		6	24	43

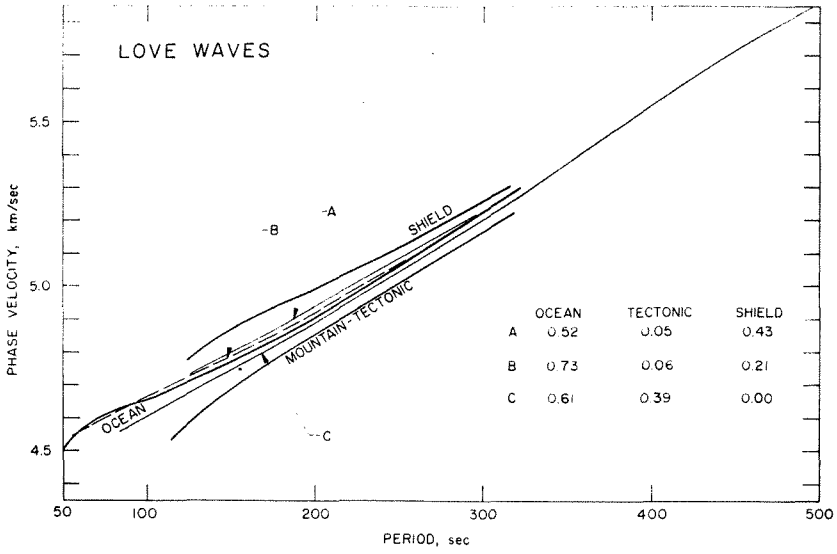

Fig. 9. Observed composite-path Love wave data and the extracted pure-path dispersion curves.

1964]. The Rayleigh wave curves were computed for this structure with a spheroidal oscillation program [*Alsop,* 1963].

For Rayleigh wave dispersion computation the compressional velocities were derived from the shear velocities using the Poisson ratios of *Gutenberg* [1959]. This was necessary because the Rayleigh wave velocities are not sensitive enough to compressional velocities to justify an independent determination of a *P* wave profile. The density model used in the dispersion calculations was determined from the linear relation between density and *P* wave velocity given by *Birch* [1961]. All three profiles—*S* wave, *P* wave, and density—have minimums in the upper mantle; the shear wave minimum is most pronounced.

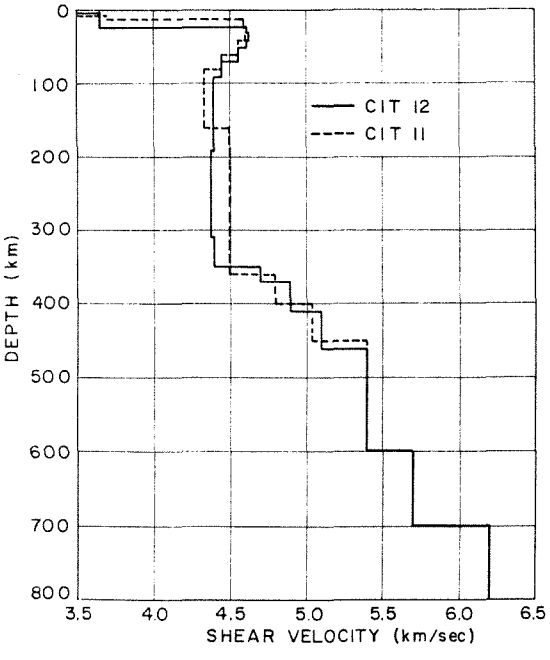

Fig. 10. Shear velocity distributions for the CIT-11 and CIT-12 mixed-path models.

The starting trial structure was model CIT 11 with a crust modified so as to represent an average of continental and oceanic conditions, namely, an 18-km crust covered with 3 km of water. The model [*Anderson and Toksöz,* 1963] was designed to satisfy data for the New Guinea–Pasadena path and was meant to represent the oceanic mantle, although the path includes about 30% shelf and continental regions. Thus CIT 11 is actually a composite model representing average conditions over the New Guinea–Pasadena path.

A model appropriate to the Mongolia–Pasadena path is designated CIT 12 [*Toksöz and Anderson,* 1963] and retains the general features noted above. The main differences (see Figure 10) are the pseudo-crust and a slightly lower average velocity in the upper 350 km. This path traverses about three times as much mountainous and tectonic terrain as the New

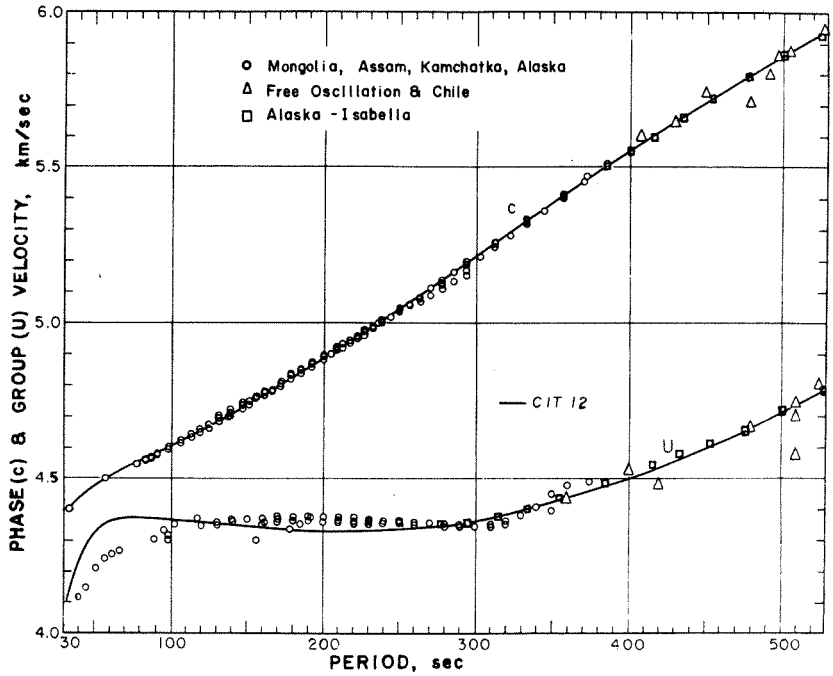

Fig. 11. Comparison of the CIT-12 Love wave dispersion curves with the observed dispersion curves from Pasadena records of the Mongolia, Assam, Kamchatka, and Alaska (1958) earthquakes and with the curves from the Isabella record of the Alaska (1964) earthquake.

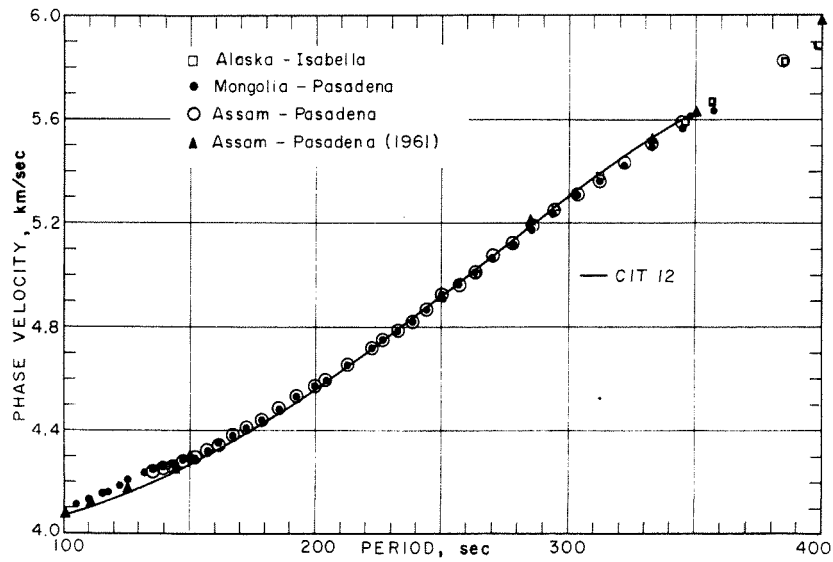

Fig. 12. Rayleigh wave dispersion curve for the CIT-12 mixed-path model and the observed data over Mongolia and Assam–Pasadena paths. The triangles are from *Brune, Nafe, and Alsop* [1961] for the same Assam–Pasadena path.

Guinea–Pasadena path, and much less shield, and the differences between the models may be due to lower average velocities in the mantle under mountains than under shields. Figures 11 and 12 give the dispersion data and the theoretical results for model CIT 12. The fit to both Love and Rayleigh waves is good.

The major characteristics of the two velocity structures can be considered to be representative features of the whole earth. These include the broad low-velocity zone extending to a depth of about 350 km, a high-velocity gradient between 350 and 450 km, and another increase in the gradients, at 600–700 km. The implication of these features, which modify the earlier concepts of the low-velocity zone and the transition region, will be discussed further in part 2.

Acknowledgments. S. S. Alexander, W. Pilant, and L. Alsop kindly furnished us with copies of their computer programs.

This research was supported by the Advanced Research Projects Agency and monitored by the Air Force Office of Scientific Research under contract AF-49(638)-1337.

References

Alsop, L. E., Free spheriodal vibrations of the earth, 1, *Bull. Seismol. Soc. Am., 53,* 483–502, 1963.

Anderson, D. L., Universal dispersion tables, 1, Love waves across oceans and continents on a spherical earth, *Bull. Seismol. Soc. Am., 53,* 681–726, 1964.

Anderson, D. L., and M. N. Toksöz, Surface waves on a spherical earth, 1, Upper mantle structure from Love waves, *J. Geophys. Res., 68,* 3483–3500, 1963.

Anderson, D. L., and M. N. Toksöz, Phase velocities of long-period surface waves and structure of the upper mantle, 2, Regional variations, in preparation, 1966.

Backus, G. E., Geographical interpretation of measurements of average phase velocities of surface waves over great circular and great semi-circular paths, *Bull. Seismol. Soc. Am., 54,* 571–610, 1964.

Birch, F., Composition of the earth's mantle, *Geophys. J., 4,* 295–311, 1961.

Brune, J. W., H. Benioff, and M. Ewing, Long-period surface waves from the Chilean earthquake of May 22, 1960, recorded on linear strain seismographs, *J. Geophys. Res., 66,* 2895–2910, 1961.

Brune, J. W., J. E. Nafe, and L. E. Alsop, The polar phase shift of surface waves on a sphere, *Bull. Seismol. Soc. Am., 51,* 247–257, 1961.

Gutenberg, B., Wave velocities below the Mohorovicic discontinuity, *Geophys. J., 2,* 348–352, 1959.

Satô, Y., Attenuation, dispersion, and the wave guide of the *G* wave, *Bull. Seismol. Soc. Am., 48,* 231–251, 1958.

Toksöz, M. N., and D. L. Anderson, Velocities of mantle Love and mantle Rayleigh waves and the structure of the earth's upper mantle, *Proj. Rept., Grant AF-AFOSR-25-63,* Seismological Laboratory, California Institute of Technology, Pasadena, May 1963.

Toksöz, M. N., and A. Ben-Menahem, Velocities of mantle Love and Rayleigh waves over multiple paths, *Bull. Seismol. Soc. Am., 53,* 741–764, 1963.

Toksöz, M. N., A. Ben-Menahem, and D. G. Harkrider, Source mechanism of Alaska earthquake from long-period seismic surface waves (abstract), *Trans. Am. Geophys. Union, 46,* 155, 1965.

(Manuscript received September 1, 1965; revised December 7, 1965.)